Pre-print version, Astrophysical Journal letters; received 2006 January 6; accepted 2006 March 2
Preprint typeset using LaTeX style emulateapj v. 6/22/04

FAR–IR EXCITED OH LINES FROM ORION KL OUTFLOWS

Javier R. Goicoechea[2], José Cernicharo[3], Mercedes R. Lerate[4,5], Fabien Daniel[3], Michael J. Barlow[5], Bruce M. Swinyard[4], Tanya L. Lim[4], Serena Viti[5], Jeremy Yates[5]

Pre-print version, Astrophysical Journal letters; received 2006 January 6; accepted 2006 March 2

ABSTRACT

As part of the first far-IR line survey towards Orion KL, we present the detection of seven new rotationally excited OH Λ–doublets (at ∼48, ∼65, ∼71, ∼79, ∼98 and ∼115 μm). Observations were performed with the *Long Wavelength Spectrometer* (LWS) Fabry–Perots on board the *Infrared Space Observatory* (ISO). In total, more than 20 resolved OH rotational lines, with upper energy levels up to ∼620 K, have been detected at an angular and velocity resolutions of ∼80″ and ∼33 km s^{-1} respectively. OH line profiles show a complex behavior evolving from pure absorption, P–Cygni type to pure emission. We also present a large scale 6′ declination raster in the OH $^2\Pi_{3/2}$ J=5/2$^+$–3/2$^-$ and $^2\Pi_{3/2}$ J=7/2$^-$–5/2$^+$ lines (at 119.441 and 84.597 μm) revealing the decrease of excitation outside the core of the cloud. From the observed profiles, mean intrinsic line widths and velocity offsets between emission and absorption line peaks we conclude that most of the excited OH arises from Orion outflow(s), i.e. the *"plateau"* spectral component. We determine an averaged OH abundance relative to H_2 of $\chi(OH)$=(0.5–1.0)×10^{-6}, a kinetic temperature of $\gtrsim$100 K and a density of $n(H_2)\simeq 5\times10^5$ cm^{-3}. Even with these conditions, the OH excitation is heavily coupled with the strong dust continuum emission from the inner *"hot core"* regions and from the expanding flow itself.

Subject headings: infrared: ISM —ISM: individual (Orion KL)—ISM: jets and outflows —ISM: molecules — radiative transfer

1. INTRODUCTION

The Kleinmann–Low (KL) infrared (IR; L∼10^5 L$_\odot$) nebula in the Orion molecular cloud is the nearest (∼450 pc) and probably the most studied massive star forming region (Genzel & Stutzki 1989). Early studies soon realized that the large scale distribution of gas and dust was heavily influenced by violent phenomena such as the interaction of compact and large scale outflows with the quiescent gas producing strong line and continuum emission. IRc2 was believed to be the main source of luminosity, heating and dynamics of the region. However, the great advances of near– and mid–IR subarcsecond resolution imaging and of (sub)millimeter interferometric observations have dramatically changed our understanding of the region. First, the 8–12 μm emission peak of IRc2 is not coincident with the Orion SiO maser origin (related to the outflow(s) origin) and second, its intrinsic IR luminosity (L∼1000 L$_\odot$) is only a fraction of the complex luminosity (Gezari et al. 1998). In addition, 3.6–22 μm images show that IRc2 is in fact resolved into four components that may even not be self–luminous. Therefore, the relevance of Irc2 as the powerful engine of Orion KL is not longer supported and its nature is now even less clear (Dougados et al. 1993; Shuping et al. 2004; Greenhill et al. 2004). A new step forward was given by Menten & Reid (1995) with the detection of the very embedded radio continuum source I (located 0″.5 south of IRc2) as the source that coincides with the centroid of the SiO maser distribution. Menten & Reid (1995) also detected the radio continuum emission of IR source n, and suggested that it could also contribute to the origin of some of the phenomena observed at larger scales. Thus, in addition to BN, the core of Orion KL contains at least two more compact HII regions (I and n) that seem to be running away from a common point, suggesting that BN, I and n were originally part of a common massive stellar system that disintegrated ∼500 years ago (Gómez et al. 2005). A causal relation between the dynamical decay of this stellar system and the observed large scale molecular outflow(s), H_2 fingers and bow shocks (Stolovy et al. 1998) has been proposed (Bally & Zinnecker 2005).

The different physical conditions and velocity fields along the line of sight result in a segregation of the gas and dust chemistry that complicates the interpretation of observations toward Orion, especially the low angular resolution molecular surveys. For this reason, it is common to distinguish between different spectral components: the *"ridge"* (extended quiescent molecular gas), the *"hot core"* (collection of very dense and hot gas clumps in which sources I and n are embedded) and the *"plateau"* (a mixture of outflow(s), shocks and interactions with the ambient cloud). Submm aperture synthesis line surveys have finally provided the spatial location and extent of many molecular species (Blake et al. 1996; Wright et al. 1996; Liu et al. 2002; Beuther et al. 2005). As a result, the formation of complex oxygen–bearing species in the interaction region between the outflow(s) and the quiescent gas is now generally understood in the context of an oxygen–rich molecular outflow (Blake et al. 1987; Wright et al. 1996; Liu et al. 2002). However, the thermal lines from basic oxygen reservoirs (O, H_2O and

[2] LERMA, UMR 8112, CNRS, Observatoire de Paris and École Normale Supérieure, 24 Rue Lhomond, 75231 Paris 05, France. (javier@lra.ens.fr)

[3] DAMIR, Instituto de Estructura de la Materia, Consejo Superior de Investigaciones Científicas, Serrano 121, 28006, Madrid, Spain. (cerni,daniel@damir.iem.csic.es)

[4] Rutherford Appleton Laboratory, Chilton, Didcot OX11 0QX, UK. (M.R.Lerate,B.M.Swinyard,T.L.Lim@rl.ac.uk)

[5] University College London, Gower Street, London WC13, UK. (mjb,sv,jyates@star.ucl.ac.uk)

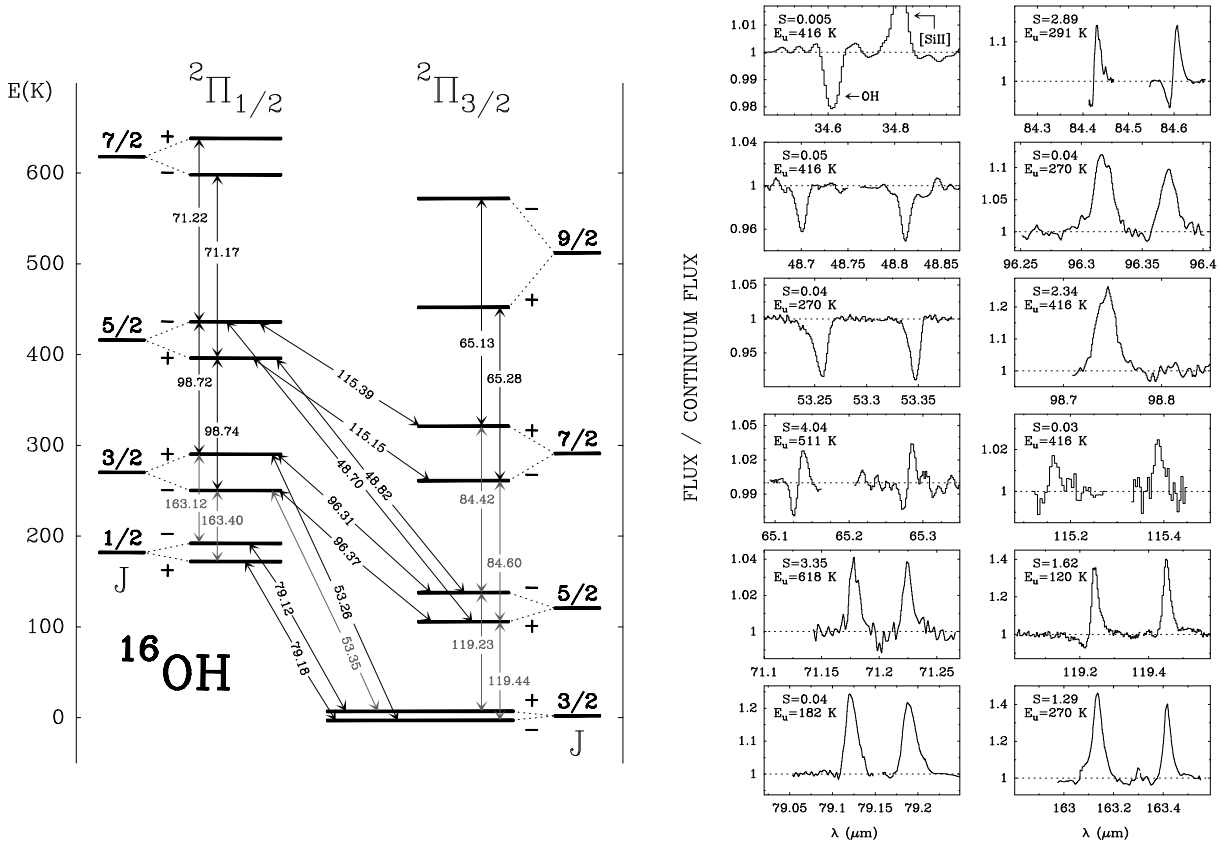

FIG. 1.— *Left:* Rotational energy diagram of ^{16}OH showing the lines detected by ISO in μm. Newly detected transitions are shown in black, while previous KAO detections are shown in grey. The $^2\Pi_{3/2}$ and $^2\Pi_{1/2}$ rotational ladders produced by the spin–orbit interaction are shown. The Λ–doubling splitting of each rotational level has been enhanced for clarity. Hyperfine structure is not shown. *Right:* ISO-LWS-FP observations of ^{16}OH towards Orion. The ordinate corresponds to the continuum normalized flux and the abscissa to the wavelength in μm. In each box, the upper level energy (in K) and the intrinsic line strength of the transition are also shown. The first box corresponds to the not resolved OH $^2\Pi_{3/2}$–$^2\Pi_{1/2}$ J=3/2–5/2 lines at ∼34 μm detected by the ISO-SWS (Wright et al. 2000).

OH) lie in the far–IR, a spectral region blocked by the earth atmosphere. Besides, the wide range of excitation conditions provided by oxygen hydrides supply unique information about the energetics and dynamics of the region. In particular, far–IR OH line emission (first detected by Storey et al. (1981)) is predicted to be a powerful diagnostic of the *plateau* gas (Draine & Roberge 1982). Observations with the *Kuiper Airborne Observatory (KAO)* allowed the detection of several low excitation OH rotational lines, see Fig. 1 (Watson et al. 1985; Viscuso et al. 1985; Betz & Boreiko 1989; Melnick et al. 1987, 1990). The specific contribution of the *hot core*, *plateau* and *ridge* components and the physical conditions within the OH emitting gas remains questionable.

2. OBSERVATIONS AND DATA REDUCTION

Most of the OH pure rotational lines appear in the wavelength range of the ISO/LWS instrument (Clegg et al. 1996). The LWS circular aperture size is ∼80″. In its Fabry–Perot mode (FP) the instrumental response is close to a Lorentzian with a spectral resolution of ∼33 km s^{-1}. In this letter we present observations that are part of the first full far–IR line survey of Orion KL using the unprecedent wavelength coverage and velocity resolution of the ISO-LWS-FP (Lerate et al. 2006, in prep.). OH spectra were obtained in the *Astronomical Observation Template* (AOT) L04 and L03 modes. Processing of the OH spectra from AOT L03 was carried out using the Offline Processing (OLP) pipeline and the LWS Interactive Analysis (LIA) package version 10. AOT L04 spectra were analyzed using the ISO Spectral Analysis Package (ISAP[5]). Typical routines include dark current optimization, deglitching and removing of the LWS grating profile, oversampling and averaging individual scans, baseline removal and line flux measurements. The full description of the complex data calibration and reduction process and associated target dedicated time numbers (TDTs) of the survey are given in Lerate et al. (2006, in prep.). The resulting OH lines are shown in Fig. 1. Finally, we present a ±180″ declination raster (see Fig. 2) in the OH $^2\Pi_{3/2}$ J=5/2$^+$–3/2$^-$ and $^2\Pi_{3/2}$ J=7/2$^-$–5/2$^+$ lines at 119.441 and 84.597 μm (L04: TDT 70101216).

3. RESULTS AND DISCUSSION

Far–IR OH lines show a complicated behavior evolving from pure absorption to pure emission profiles. The detection of P-Cygni type profiles in $^2\Pi_{3/2}$ OH excited rotational lines at ∼65 and ∼84 μm (Fig. 1) and in the ^{18}OH ground–state line (Fig. 2; also detected by

[5] ISAP is a joint development by the LWS and SWS Instruments Teams and Data Centers. Constributing institutes are CESR, IAS, IPAC, MPE, RAL and SRON.

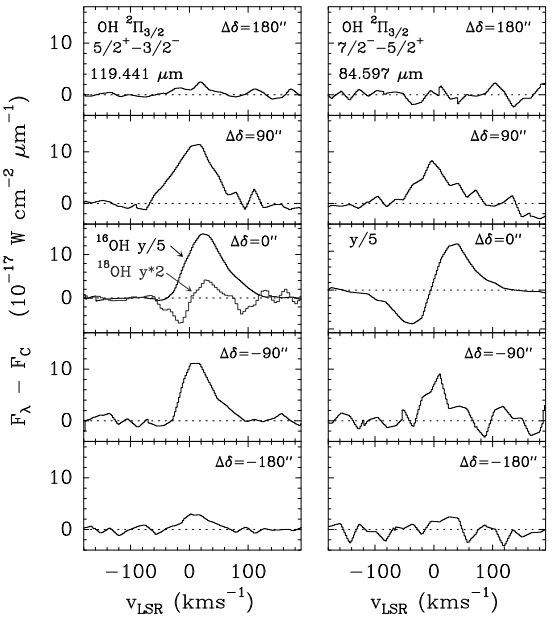

FIG. 2.— Continuum subtracted ISO–LWS–FP spectra taken at different declination offsets from Orion IRc2. Offsets in arcsec are indicated. The left (0″,0″) panel shows the different ground–state line profiles produced by ^{16}OH and ^{18}OH (also detected by KAO).

KAO; Melnick et al. 1990) confirms that most of the OH emission arises from an extended molecular outflow. Since its optical depth is small, the ^{18}OH emission helps to trace the dominant outflow origin of the OH emission. Compared with stellar wind profiles, the molecular far–IR P–Cygni type profiles are favored by the presence of far–IR (dust) continuum emission throughout the expanding flow (and not only from a central continuum source). Hence, the detailed balance between emission and absorption components critically depends on the dust and OH emissivities, opacities and beam filling factors at each wavelength. Simple nonlocal non–LTE radiative transfer models for dust and OH easily reproduce these characteristics (see below). On the other hand, all observed OH lines within the $^2\Pi_{1/2}$ ladder (∼71, ∼98 and ∼163 μm) appear in emission with a peak velocity of $v \gtrsim +15$ km s^{-1} showing less indication of self–absorption (the cloud rest velocity is ∼9 km s^{-1}; Scoville et al. (1983)). Taking into account the high energy of the associated levels, effective radiative pumping by the far–IR dust continuum emission must be playing a role in the OH excitation. This is clearly favored by the detection of several $^2\Pi_{3/2}$–$^2\Pi_{1/2}$ cross–ladder transitions in almost pure absorption (∼34, ∼48 and ∼53 μm). Hence, temperatures and densities in the outflow can be significantly lower than those required to thermalise the OH emission lines. Other newly detected OH excited cross–ladder transitions (∼96 and ∼115 μm) are observed in pure emission and they contribute to the radiative de–excitation of associated $^2\Pi_{1/2}$ upper levels. Note that the absorption peak of pure absorption OH lines occurs at negative velocities, $v \lesssim -15$ km s^{-1}. Similar conclusions apply for water lines (Cernicharo et al. 1999a). In particular, pure absorption mid–IR H_2O lines peak at -8 ± 3 km s^{-1} (Wright et al. 2000). Taking into account the velocity resolution and wavelength calibration of the LWS/FP instrument, we find 25±5 km s^{-1} as the most likely expansion velocity of the far–IR OH flow. The inferred expansion velocity seems more consistent with the 18±2 km s^{-1} *low–velocity outflow*, originally revealed by water maser motions (Genzel et al. 1981). In addition, it is known that OH 1.6 GHz masers toward the Orion KL region are detected over an area of 30″ in diameter. The best kinematical model fitting the OH maser emission is found for an uniform expansion velocity of 21.0±3.5 km s^{-1} away from a source (at or near IRc2) with a radial velocity of 9.0±0.5 km s^{-1} (Cohen et al. 2006). Contribution from the extended *high–velocity outflow* (Martín-Pintado et al. 1990) could also be present (see predictions by Melnick et al. 1990). Only the OH ground–state lines at ∼119 μm show high–velocity broad–red–wing emission above ∼100 km s^{-1}. This high–velocity emission is not observed in any other OH line by ISO.

The large–scale OH declination raster clearly shows that OH lines are weaker (at least by a factor of 5) outside the central position (Fig. 2). This is likely due to lower excitation (continuum emission and densities decrease) in the extended cloud, but not necessarily to a steep decrease of OH abundance in the *ridge*. Unfortunately, it is impossible to infer the exact spatial distribution of the newly detected OH lines from the large ISO beam. KAO heterodyne observations of the ∼119.2 μm line (with a beam of ∼33″) showed that OH emission may be spatially compact. Betz & Boreiko (1989) deduced that the OH emission comes from a source <25″ in full–width at half–maximum diameter. Therefore, the same inner regions of the large scale outflow revealed by H_2O masers at ∼325 GHz (Cernicharo et al. 1999b), and HDO emission at ∼893 and ∼850 GHz (Pardo et al. 2001). Besides, OH may also arise from the regions where the outflow plunge into the quiescent cloud producing dissociative shocks. According to recent [C I] observations (with 10″ angular resolution), molecular dissociation occurs in a shell of ∼40″ diameter (Pardo et al. 2005), therefore within the LWS beam. Nevertheless, the OH emission measured by Betz & Boreiko (1989) towards the bright H_2 shocked regions Peak 1/2 is significantly weaker than towards the outflow itself. More quantitative conclusions about the spatial distribution of the OH flow require much higher angular resolution observations.

In order to estimate the OH abundance and the physical conditions leading to the observed line profiles, we have modeled the first 20 OH rotational levels with the nonlocal code used in our OH study of Sgr B2 (Goicoechea & Cernicharo 2002). We have modeled a spherical shell with a 25″ diameter expanding at 25 km s^{-1} that surrounds an uniform core, optically thick in the far–IR, with a 10″ diameter and a color temperature of 150 K. These values agree with those obtained from high dipole molecules towards the *hot core*. In all models, the dust emission reasonably fits the far–IR continuum levels measured by the LWS. Obviously this model simplifies the inhomogeneous and clumpy nature of the region as ISO observations average all the sub–structure morphology and the different physical conditions found in the *plateau*. In our view, the far–IR OH excited emission may be spatially associated with the SO

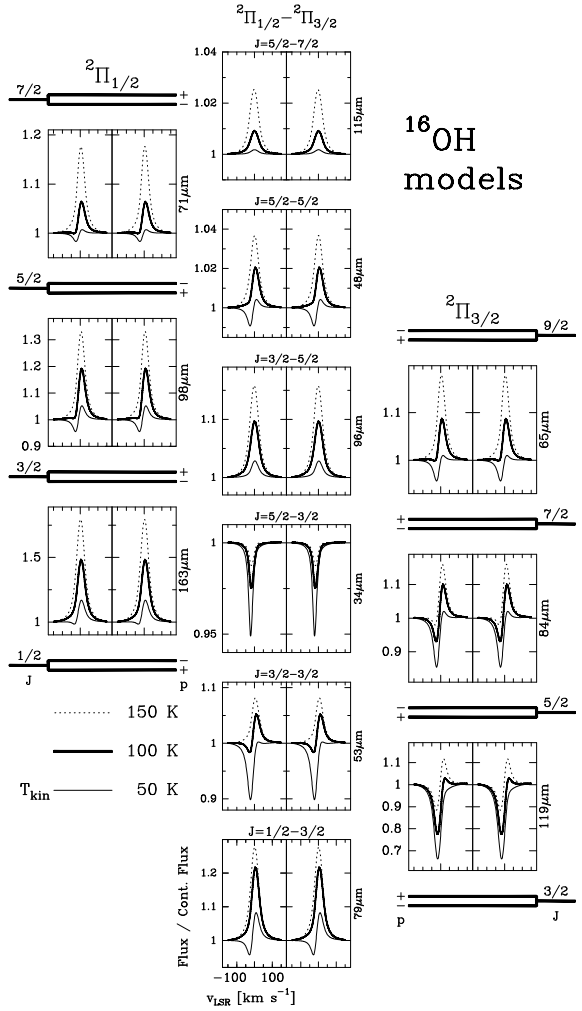

FIG. 3.— Radiative transfer models for an expanding OH shell. Common parameters are: χ(OH)=5×10^{-7} and $n(H_2)$=5×10^5 cm^{-3}. Three different temperatures are considered: T_k = 50, 100, and 150 K. Each panel correspond to a rotational Λ–doublet. The wavelength of each transition is shown. Line profiles have been convolved with a gaussian beam of 80″ and with a spectral resolution Lorentzian width of 33 km s^{-1}.

and SO_2 shell of low–velocity expanding gas, observed at ∼1″ resolution, where the outflow shocks dense clumps of ambient material (Wright et al. 1996).

A grid of models has been generated by varying T_k=T_{dust} from 50 to 250 K, $n(H_2)$ from 10^5 to 10^7 cm^{-3} and χ(OH) from 10^{-8} to 10^{-5} in the outflow. The newly detected OH excited lines add some important constraints into the *plateau* physical conditions. Basically, the fact that excitation temperatures in several excited OH cross–ladder transitions have to be below T_{dust} constraints the maximum T_k and $n(H_2)$ allowed to produce absorption in these transitions. These absorptions can only be reproduced if $n(H_2)$<5×10^6 cm^{-3}, otherwise collisional excitation and re–emission dominates. For this range of $n(H_2)$, the bulk of gas has to be above T_k=50 K, otherwise absorption will dominate the lower energy cross–ladder and $^2\Pi_{3/2}$ intra–ladder transitions. On the other hand, collisional excitation will dominate for T_k>200 K. Since high T_k and $n(H_2)$ conditions result in a OH pure emission line spectrum, a dominant contribution from the *hot core* is not expected. In addition, the large far–IR line+continuum opacity in the *plateau* itself will hide most of the *hot core* OH emission. The lack of spectral resolution makes a more accurate analysis of possible absorptions impossible.

Nevertheless, the detected OH self–absorptions and P–Cygni type profiles allows one to constraint the physical parameters leading to the observed balance between collisions and radiative pumping. The best single–component fit to the OH observations is obtained around T_k∼100 K and $n(H_2)$∼5×10^5 cm^{-3} (see models in Fig. 3). In comparison with far–IR H_2O ground–state or CO high–J lines, OH cross–ladder transitions have both small spontaneous emission rates and small line strengths. In most applications this indicates that the associated far–IR lines are optically thin. The lack of opacity broadening also implies that their line profiles are more sensitive to gas velocity fields and turbulence. A good agreement with observations is found for χ(OH)=(0.5–1.0)×10^{-6}. Therefore, *ISO* observations clearly show that OH is very abundant in the *plateau*. These results provide additional insights to the fact that complex O–rich molecules such as methanol (CH_3OH) (Wright et al. 1996) or formid acid (HCOOH) (Liu et al. 2002) are specifically enhanced (when resolved at much higher resolution) in the interaction surfaces between the outflow (OH rich) material and the ambient cloud. Only the wide range of excitations provided by water lines and the input from chemical models, able to predict the chemistry evolution of the physically distinct regions in Orion, can extract more accurate information from far–IR observations.

We are grateful to the LWS instrument and the ISO data base teams for the quality of the provided data. The referee help us to improve our high resolution view of Orion. JRG was supported by a *Marie Curie Intra-European Individual Fellowship* within the 6th European Community Framework Programme, contract MEIF–CT–2005–515340. We thank the Spanish DGES and PNIE grants ESP2001-4516 and AYA2003-2785.

REFERENCES

Bally, J. & Zinnecker, H. 2005, AJ, 129, 2281
Betz, A. L. & Boreiko, R. T. 1989, ApJ, 346, L101
Beuther, H. et al. 2005, ApJ, 632, 355
Blake, G. A., Sutton, E.C., Masson, C. R., & Phillips, T. G. 1987, ApJ, 315, 621
Blake, G.A. et al. 1996, ApJ, 472, L49
Cernicharo et al. 1999a, The Universe as Seen by ISO. Eds. P. Cox & M. F. Kessler. ESA-SP 427, p. 565.
Cernicharo, J. et al. 1999b, ApJ, 520, L131
Clegg, P.E., et al. 1996, A&A, 315, L38
Cohen, R. J., Gasipron, N., Meaburn, J. & Graham, M. F. 2006, MNRAS, in press.
Dougados, C., Lena, P., Ridgway, S. T., Christou, J. C., & Probst, R. G. 1993, ApJ, 406, 112
Draine, B. T., & Roberge, W. G. 1982, ApJ, 259, L91
Genzel, R., & Stutzki, J. 1989, ARA&A, 27, 41
Genzel, R., Reid, M. J., Moran, J. M., & Downes, D. 1981, ApJ, 244, 884
Gezari, D. Y., Backman, D. E., & Werner, M. W. 1998, ApJ, 509, 283

Goicoechea, J.R., & Cernicharo, J. 2002, ApJ, 576, L77
Gómez, L., Rodríguez, L.F., Loinard, L., Lizano, S., Poveda, A., & Allen, C. 2005, ApJ, 635, 1166
Greenhill, L. J., Gezari, D. Y., Danchi, W. C., Najita, J., Monnier, J. D., & Tuthill, P. G. 2004, ApJ, 605, L57
Martín-Pintado, J., Rodríguez-Franco, A., & Bachiller, R. 1990, ApJ, 357, L49
Melnick, G. J., Genzel, R., & Lugten, J. B. 1987, ApJ, 321, 530
Melnick, G. J., Stacey, G. J., Lugten, J. B., Genzel, R., & Poglitsch, A. 1990, ApJ, 348, 161
Menten, K.M. & Reid, M.J. 1995, ApJ, 445 L157
Liu, S.Y., Girart, J.M., Remijan, A. & Snyder, L. E. 2002, ApJ, 576, 255
Pardo, J.R., Cernicharo, J., Herpin, F., Kawamura, J., Kooi, J., & Phillips, T.G. 2001, ApJ, 562, 799
Pardo, J.R., Cernicharo, J. & Phillips, T.G. 2005, ApJ, 634, L61
Scoville, N., Kleinmann, S. G., Hall, D. N. B. & Ridgway, S. T. 1983, ApJ, 275, 201
Storey, J. W. V., Watson, D. M., & Townes, C. H. 1981, ApJ, 244, L27
Stolovy, S. R. et al. 1998, ApJ, 492, L151
Shuping, R. Y., Morris, M., & Bally, J. 2004, AJ, 128, 363
Viscuso, P. J., Stacey, G. J., Harwit, M., Haas, M. R., Erickson, E. F., & Duffy, P. B. 1985, ApJ, 296, 149
Watson, D. M., Genzel, R., Townes, C. H., & Storey, J. W. V. 1985, ApJ, 298, 316
Wright, M. C. H., Plambeck, R. L. & Wilner, D. J. 1996, ApJ, 469, 216
Wright, C. M., van Dishoeck, E. F., Black, J. H. et al. 2000, A&A, 358, 689